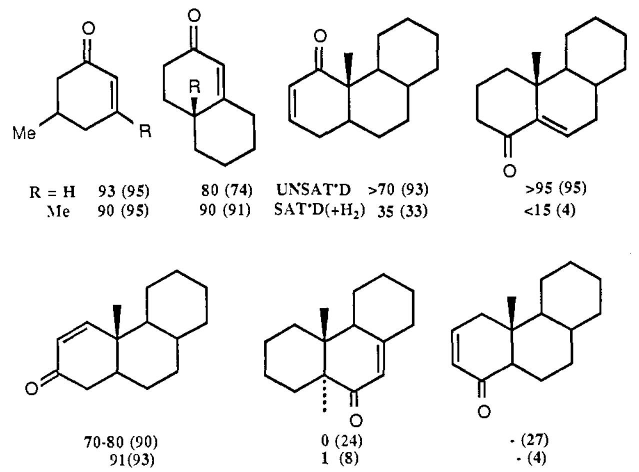

Figure 2. Experimental[4] (calculated) percentages of axial attack on cyclohexanones and cyclohexenones.

the coplanarity restraint of the enone, the predicted stereochemistry resembles that of the analogous cyclohexanones.

Figure 1 shows Newman projections sighting along the C_2C_1 bond of cyclohexanone, **1**, and 2-cyclohexenone, **2**, and of the transition states for axial and equatorial attack by hydride on these species. Even in the reactants, it is clear that the introduction of a double bond has greatly modified the dihedral angles along these bonds. In particular, the "internal dihedral", marked θ_i in the drawings, has decreased from its value of 51° in cyclohexanone to 22° in 2-cyclohexenone. This geometrical change results in a pronounced difference in torsional interactions upon axial and equatorial attack, which are designated qualitatively by arrows drawn perpendicular to the carbonyl plane in the drawings **1** and **2** in Figure 1.

The modified MM2 force field predicts that structures **3** and **5** in Figure 1 differ in energy by 1.2 kcal/mol, implying that the axial/equatorial attack ratios for hydride reduction of simple cyclohexanones should be 88:12 at 25°. Experimentally, these are 84–97:16–3.[2] Axial attack on cyclohexanone, **3**, occurs with less eclipsing of the forming H–C bond as compared to equatorial attack, **5**, as proposed by Felkin. With cyclohexenone, the difference between axial attack **4** and equatorial attack **6** is even more pronounced. Therefore, the axial/equatorial energy difference increases from 1.2 kcal/mol between **3** and **5** to 2.0 kcal/mol between **4** and **6**. At 25°, this corresponds to a 97:3 ratio.

How does this rationalization compare with the alternative proposals by Toromanoff and Baldwin? Our model indicates that overlap of the forming bond with the adjacent π bond is maintained upon axial attack as proposed by Toromanoff. However, the overlap is also maintained upon equatorial attack but is accompanied by severe torsional problems.

Baldwin proposed that the approach vector is different in ketones and α,β-unsaturated ketones.[4] The proposed approach vectors for cyclohexanone and cyclohexenone are shown in **7** and **8**. Our computations provide no support for this contention.

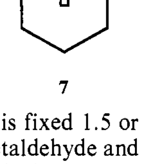

7

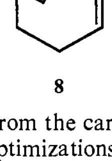

8

When a hydride is fixed 1.5 or 2 Å from the carbonyl carbon of acrolein or of acetaldehyde and full optimizations are carried out, a 0–3° tilt of hydride toward hydrogen is found. Furthermore, our force field model, which predicts no alteration of approach vector in unsaturated ketones, gives excellent semiquantitative agreement with experimental LAH stereoisomer ratios for reactions of a variety of cyclohexanones and the corresponding cyclohexenones (see Figure 2).

Although for rigid cyclohexenones, the stereoselectivity is higher than for rigid cyclohexanones, cyclohexenones with small alkyl substituents may react with low stereoselectivity. For example, our model predicts that 4-methyl-2-cyclohexenone will react with low selectivity, since the transition state with a quasi-axial 4-methyl substituent is only 0.7 kcal/mol higher in energy than that with a quasi-equatorial 4-methyl group.

To verify that the differences in selectivity really can arise from changes in staggering about the C_1C_2 bond, we calculated the rotational barrier about the single bond of acetone in the ab initio transition structure for the addition of lithium hydride to acetone.[2a] Although the H---C bond is only partially formed, the rotational barrier is 3.2 kcal/mol by these calculations. This is more than enough to indicate that the energy differences among the transition structures **3**–**6** can be accounted for by torsional effects. This applies to hydride, acetylide, and cyanomethyl anion additions.

In summary, we have found that the high stereoselectivity in nucleophilic additions of unhindered nucleophiles to cyclohexenones can be accounted for quantitatively in terms of a torsional model such as proposed by Felkin to rationalize cyclohexanone stereoselectivities.[2c]

Acknowledgment. We are grateful to the National Institutes of Health for financial support of this research.

The Crystal Structures of Two Cesides Show That Cs$^-$ Is the Largest Monotomic Ion

Rui H. Huang, Donald L. Ward, Mark E. Kuchenmeister, and James L. Dye*

Department of Chemistry and Center for Fundamental Materials Research
Michigan State University
East Lansing, Michigan 48824

Received April 21, 1987

Although we have synthesized over 30 alkalides and eight electrides since the first sodide $Na^+(C222){\cdot}Na^-$ (C222 = cryptand[2.2.2]) was prepared in 1974,[1,2] only recently have suitable crystal-growing and -handling techniques been developed for single-crystal structure determinations.[3,4] The ceside, $Cs^+(18C6)_2{\cdot}Cs^-$ (I) (18C6 = 18-crown-6) was characterized by optical and solid-state NMR methods.[5-8] Polycrystalline samples of a second ceside, $Cs^+(C222){\cdot}Cs^-$ (II), were first thought to contain no ceside anions because the expected Cs^- peak was not seen in the ^{133}Cs MAS–NMR spectrum.[9] We report here the crystal structures of both cesides, which permit assignment of an effective average radius of 3.5 Å for Cs^- and which may explain the presence of a Cs^- NMR peak in I and its absence in II.

Polycrystalline samples were prepared as previously described.[10] Saturated solutions in dimethyl ether–trimethylamine mixtures which contained a number of seed crystals were cooled from −45

---

(1) Dye, J. L.; Ceraso, J. M.; Lok, M. T.; Barnett, B. L.; Tehan, F. J. *J. Am. Chem. Soc.* **1974**, *96*, 608–609.

(2) Tehan, F. J.; Barnett, B. L.; Dye, J. L. *J. Am. Chem. Soc.* **1974**, *96*, 7203–7208.

(3) Ward, D. L.; Dawes, S. B.; Fussa, O.; Dye, J. L. *Abstracts American Crystallographic Association Proceedings, Series 2*; 1985, Vol. 13, p 25.

(4) Dawes, S. B.; Ward, D. L.; Huang, R. H.; Dye, J. L. *J. Am. Chem. Soc.* **1986**, *108*, 3534–3535.

(5) Ellaboudy, A.; Dye, J. L. *J. Am. Chem. Soc.* **1983**, *105*, 6490–6491.

(6) Dye, J. L.; Ellaboudy, A. *Chem. Br.* **1984**, *20*, 210–215.

(7) Dye, J. L. *Prog. Inorg. Chem.* **1984**, *32*, 327–441.

(8) Issa, D.; Ellaboudy, A.; Janakiraman, R.; Dye, J. L. *J. Phys. Chem.* **1984**, *88*, 3847–3851.

(9) Ellaboudy, A. S. Ph.D. Dissertation, Michigan State University, East Lansing, MI, 1984.

(10) Dye, J. L. *J. Phys. Chem.* **1984**, *88*, 3842–3846.

0002-7863/87/1509-5561$01.50/0 © 1987 American Chemical Society

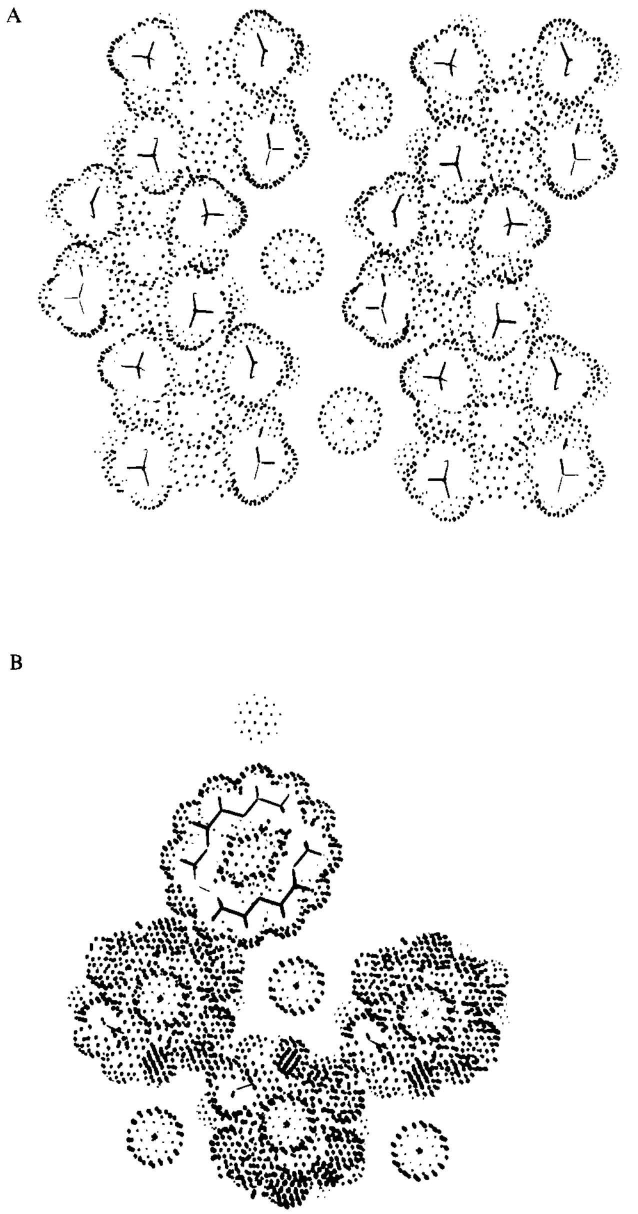

Figure 1. Two thin sections of the $Cs^+(18C6)_2 \cdot Cs^-$ structure with Cs^- locations represented by the isolated circular patterns. The *a*-axis is directed to the right: (A) *b*-axis up and (B) view down the *b*-axis through the center Cs^- of view A, *c*-axis up.

to −60 °C over a 10-h period. The mother liquor was removed by pouring and vacuum distillation at −60 °C. The dry, cold crystals, shiny bronze in color, were transferred in a nitrogen-filled glovebag into a rectangular depression in a copper block, kept at −50 °C, and covered with cold, purified *n*-octane. This protection from the glovebag atmosphere permitted selection of well-formed crystals by microscopic examination. Suitable crystals were removed from the cold octane by a glass fiber with vacuum grease on its tip and transferred in a stream of −60 °C nitrogen gas onto a Nicolet P3F diffractometer. During X-ray data collections, the crystals were kept in a cold (−70 to −80 °C) nitrogen gas stream to prevent thermal decomposition and oxidation. As with most other alkalides, these compounds react readily with air and moisture and decompose irreversibly above ~ −20 °C.

The structure of $Cs^+(18C6)_2 \cdot Cs^-$ was solved by using the Patterson heavy atom method to reveal the positions of the two cesium ions, while that of $Cs^+(C222) \cdot Cs^-$ was solved by direct methods in which the two cesium ions were located from an E-map. In both cases, difference Fourier syntheses revealed the remaining atoms. Hydrogen atoms were included but constrained to ride on the atom to which they were bonded. Final agreement factors were $R = 0.041$ and $R_w = 0.041$ (I) and $R = 0.071$ and $R_w = 0.057$ (II). The crystallographic data are given in Table I. Complete data are given in the Supplementary Material.

Table I. Crystallographic Data for Two Cesides[a]

	$Cs^+(18C6)_2 \cdot Cs^-$	$Cs^+(C222) \cdot Cs^-$
space group	*Pbca*	$P2_1/n$
cell params	$a = 16.212\ (8)$ Å $b = 16.374\ (6)$ Å $c = 31.315\ (14)$ Å	$a = 13.371\ (2)$ Å $b = 11.252\ (2)$ Å $c = 21.529\ (3)$ Å $\beta = 94.80\ (1)°$
	$V = 8312\ (6)$ Å^3 $Z = 8$	$V = 3227.7\ (9)$ Å^3 $Z = 4$
no. of reflecns collctd	6585	4702
no. of unique reflcns	5413	4211
no. of reflcns used in refnmnt	2221 with $F_o^2 > 3\sigma(F_o^2)$	1418 with $F_o^2 > 2\sigma(F_o^2)$

[a] max $2\theta = 45°$.

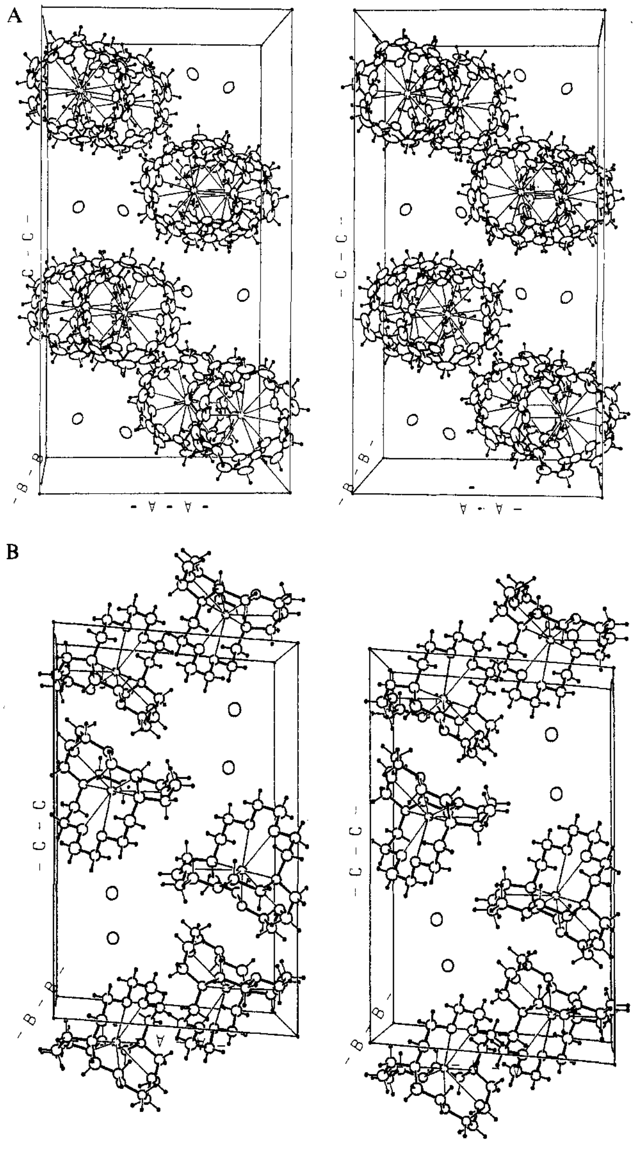

Figure 2. ORTEP stereo packing diagrams of (A) $Cs^+(18C6)_2 \cdot Cs^-$ and (B) $Cs^+(C222) \cdot Cs^-$.

In both structures, the cesium anions are in pockets lined with H atoms from the crown ethers or cryptands. The closest Cs^-–H distances are 4.29 Å (I) and 4.37 Å (II). The average distances to the 15 closest atoms (all are H atoms) are 4.66 Å (I) and 4.70 Å (II). A hydrogen van der Waals radius of 1.2 Å yields a

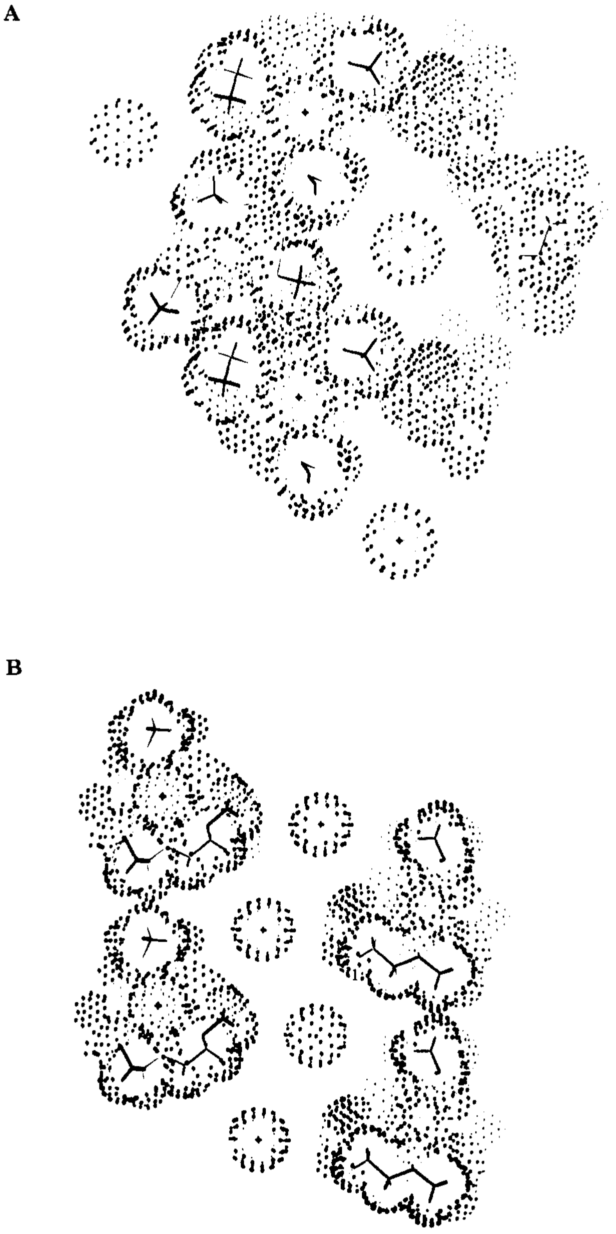

Figure 3. Two thin sections of the $Cs^+(C222)\cdot Cs^-$ structure with Cs^- locations represented by the isolated circular patterns. The *c*-axis is directed to the right: (A) *b*-axis up and (B) view down the *b*-axis at the second Cs^- from the top in view A, *a*-axis down.

minimum radius for Cs^- of 3.1 Å. We expect Cs^- to be rather polarizable so that H atoms might penetrate somewhat into the outer electron density. The average distance to neighboring H atoms yields an effective radius of 3.5 Å showing that Cs^- occupies more than 4 times the volume of I^-!

In $Cs^+(18C6)_2\cdot Cs^-$, the cesium cation is coordinated to the 12 oxygen atoms of two sandwich-forming crown ether molecules with Cs^+–O distances ranging from 3.113 (7) Å to 3.516 (7) Å. The average distance of 3.31 Å is close to those in $Cs^+(18C6)_2\cdot Na^-$ [3.36 Å][3] and in $Cs^+(18C6)_2\cdot e^-$ [3.35 Å].[4] Thus, except for small conformational effects, the nature of the sandwich-complexed cesium cation seems independent of the anion. The inclusive cesium cation in $Cs^+(C222)\cdot Cs^-$ has six Cs^+–O distances ranging from 2.888 (15) Å to 2.99 (2) Å, with two nitrogen atoms at 3.07 (2) Å. Its structure is very similar to that in $Cs^+(C222)\cdot SCN^-\cdot H_2O$.[11]

Whereas close packing of the large complexed cations in $Cs^+(18C6)_2\cdot Na^-$ and $Cs^+(18C6)_2\cdot e^-$ leads to "natural" anionic vacancies, with each anion surrounded by eight cations, the large size of Cs^- in $Cs^+(18C6)_2\cdot Cs^-$ gives much more complicated packing. Both the cations and the anions form zigzag chains parallel to the *b*-axis [displacements, ±1.59 Å (Cs^+) and ±1.69 Å (Cs^-)] with uniform interionic distances of 8.78 and 8.86 Å, respectively. Each Cs^- is also 8.12 Å from another Cs^- in an adjacent chain. The "coordination shell" of each Cs^- is completed by seven complexed cations at distances of 8.09, 8.30, 8.31, 8.45, 9.28, 9.52, and 9.65 Å. Two views of the packing are shown in Figure 1, and a stereo ORTEP view of the unit cell is given in Figure 2A.

The most striking feature of the ion packing in $Cs^+(C222)\cdot Cs^-$ is the very short, uniform Cs^- to Cs^- distance of 6.38 Å in zigzag chains parallel to the *b*-axis (displacements, ±1.50 Å) showing that the anions are in contact. The resulting strong perturbation from spherical symmetry may mix enough 5d character into the ground-state 6s wave function to give substantial anisotropic spin-orbit coupling, which would broaden the powder ^{133}Cs NMR signal beyond detection limits.[9]

In addition to the two adjacent anions in the chain, each Cs^- has nine neighboring cryptated Cs^+ ions at 7.13, 8.10, 8.60, 8.83, 8.89, 8.97, 8.97, 9.11 and 9.11 Å. The nearest Cs^- in an adjacent chain is at 10.03 Å. Two views of the packing are shown in Figure 3, and a stereo ORTEP drawing of the unit cell is shown in Figure 2B.

Acknowledgment. This work was supported by National Science Foundation Solid State Chemistry Grant DMR 84-14154, and the X-ray diffractometer system was provided by NSF Grant CHE 84-03823. Partial support for this research was obtained from the Michigan State University Center for Materials Research. We are grateful to Dr. David A Liberman of the Lawrence Livermore National Laboratory for calculating the alkalide atomic scattering factors and for permission to use them in a publication.

Supplementary Material Available: Tables of data collection and refinement summaries, positional parameters, thermal parameters, bond distances and angles, and an appendix that describes atomic scattering factors for X-rays for Li^-, Na^-, K^-, Rb^-, and Cs^- (42 pages); tables of observed and calculated structure factors (116 pages). Ordering information is given on any current masthead page.

---

(11) Moras, P.; Metz, B.; Weiss, R. *Acta Crystallogr., Sect. B: Struct. Crystallogr. Cryst. Chem.* **1973**, *B29*, 388-395.